Supplementary Materials

Materials and Methods

PathScan® RTK Signaling Antibody Array Kit Target Map (Cell Signaling)

+	+	4	4	9	9	14	14	+	19	19	24	24	29	29	34	34	+
1	1	5	5	10	10	15	15	+	20	20	25	25	30	30	35	35	+
2	2	6	6	11	11	16	16	-	21	21	26	26	31	31	36	36	39
3	3	7	7	12	12	17	17	-	22	22	27	27	32	32	37	37	39
+	+	8	8	13	13	18	18	+	23	23	28	28	33	33	38	38	+

1. **EGFR/ErbB1 pan-Tyr**
2. **HER2/ErbB2 pan-Tyr**
3. **HER3/ErbB3 pan-Tyr**
4. **FGFR1 pan-Tyr**
5. **FGFR3 pan-Tyr**
6. **FGFR4 pan-Tyr**
7. **InsR pan-Tyr**
8. **IGF-IR pan-Tyr**
9. **TrkA/NTRK1 pan-Tyr**
10. **TrkB/NTRK2 pan-Tyr**
11. **Met/HGFR pan-Tyr**
12. **Ron/MST1R pan-Tyr**
13. **Ret pan-Tyr**
14. **ALK pan-Tyr**
15. **PDGFR pan-Tyr**
16. **c-Kit/SCFR pan-Tyr**
17. **FLT3/Flk2 pan-Tyr**
18. **M-CSFR/CSF-1R pan-Tyr**
19. **EphA1 pan-Tyr**
20. **EphA2 pan-Tyr**
21. **EphA3 pan-Tyr**
22. **EphB1 pan-Tyr**
23. **EphB3 pan-Tyr**
24. **EphB4 pan-Tyr**
25. **Tyro3/Dtk pan-Tyr**
26. **Axl pan-Tyr**
27. **Tie2/TEK pan-Tyr**
28. **VEGFR2/KDR pan-Tyr**
29. **Akt/PKB/Rac Thr308**
30. **Akt/PKB/Rac Ser473**
31. **p44/42 MAPK (ERK1/2) Thr202/Tyr204**
32. **S6 Ribosomal Protein Ser235/236**
33. **c-Abl pan-Tyr**
34. **IRS-1 pan-Tyr**
35. **Zap-70 pan-Tyr**
36. **Src pan-Tyr**
37. **Lck pan-Tyr**
38. **Stat1 Tyr701**
39. **Stat3 Tyr705**

***Note: + indicates positive control lane**
- indicates negative control lane

Antibodies and Other Reagents

Reagent		Company	Catalogue Number
Heregulin beta-1 human		Sigma-Aldrich	SRP3055
EGF Recombinant Human Protein		Gibco, Life Technologies	PHG0311
PF-562271 (29)		AdooQ Bioscience	A11192
PF-573228 (28)		AdooQ Bioscience	A11235
PF-04554878 (VS-6063, Defactinib) (46)		AdooQ Bioscience	A11929
FAK siRNA (GCUAGUGACGUAUGGAUGU)		Sigma	n/a
siRNA Universal Negative Control #1		Sigma	SIC001
Location	**Antibody**	**Company**	**Catalogue Number**
FAK: N-terminal	Anti-FAK Antibody, clone 4.47	EDM Millipore	05-537
FAK: C-terminal	Anti-FAK antibody [63D5]	abcam	ab72140
FAK: Y397	Phospho-FAK (Tyr397) Antibody	Cell Signaling Technologies	3283
EGFR: Y1068	Phospho-EGF Receptor (Tyr1068) (D7A5) XP® Rabbit mAb	Cell Signaling Technologies	3777
EGFR: Intracellular Domain	EGF Receptor (D38B1) XP® Rabbit mAb	Cell Signaling Technologies	4267
HER2: Y1248	Phospho-HER2/ErbB2 (Tyr1248) Antibody	Cell Signaling Technologies	2247
HER2: Intracellular Domain	HER2/ErbB2 (29D8) Rabbit mAb	Cell Signaling Technologies	2165
HER2: Extracellular Domain	HER2/ErbB2 (D8F12) XP® Rabbit mAb	Cell Signaling Technologies	4290
AKT: S473	Phospho-Akt (Ser473) Antibody	Cell Signaling Technologies	9271
AKT: C-terminal	Akt Antibody	Cell Signaling Technologies	9272
ERK: T202/Y204	Phospho-p44/42 MAPK (Erk1/2) (Thr202/Tyr204) Antibody	Cell Signaling Technologies	9101
ERK: C-terminal	p44/42 MAPK (Erk1/2) Antibody	Cell Signaling Technologies	9102
GAPDH: Full Length	GAPDH Antibody (ZG003)	Invitrogen	39-8600
β-Actin: N-terminal	Monoclonal Anti-β-Actin antibody produced in mouse	Sigma Aldrich	A5441

Supplementary Figures

Fig. # S1:

A MDA-MB-453 Quantification

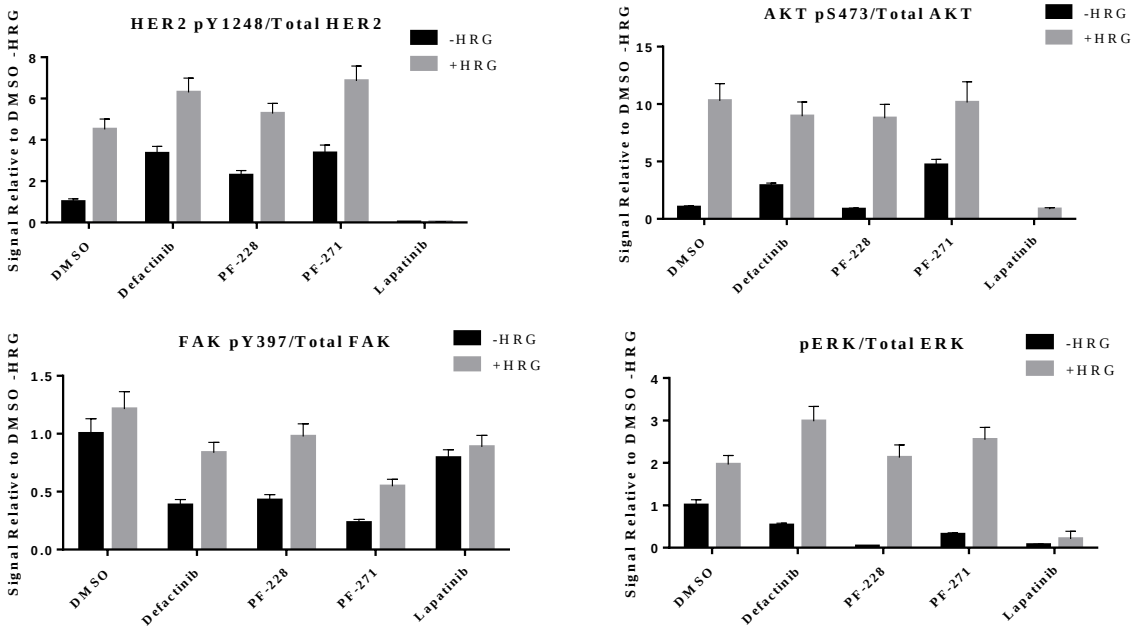

B SkBr3 Quantification

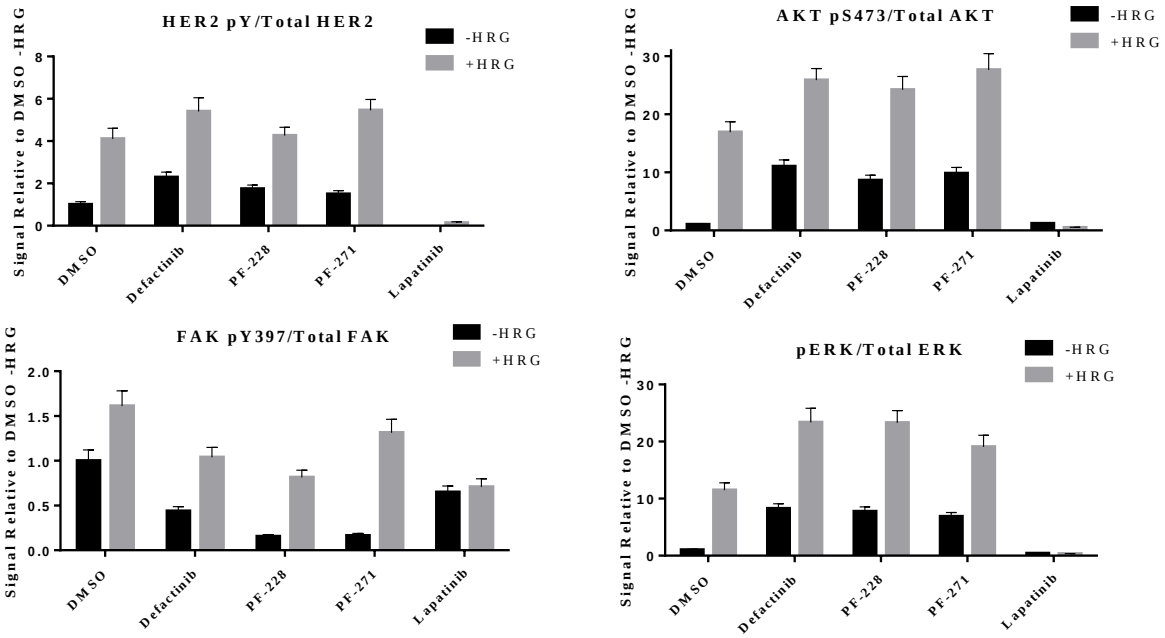

Fig. S1. Quantification of MDA-MB-453 and SkBr3 immunoblot experiments from Fig. 1. Densitometry analysis from experiments in HER2-positive **(A)** MDA-MB-453 and **(B)** SkBr3 breast cancer cells relative to DMSO –HRG control. Results shown are averaged results from three independent experiments, with error bars represented as standard deviations. Two-way ANOVA statistical analysis is shown in Supplemental File 2.

Fig. # S2:

A H292 Quantification

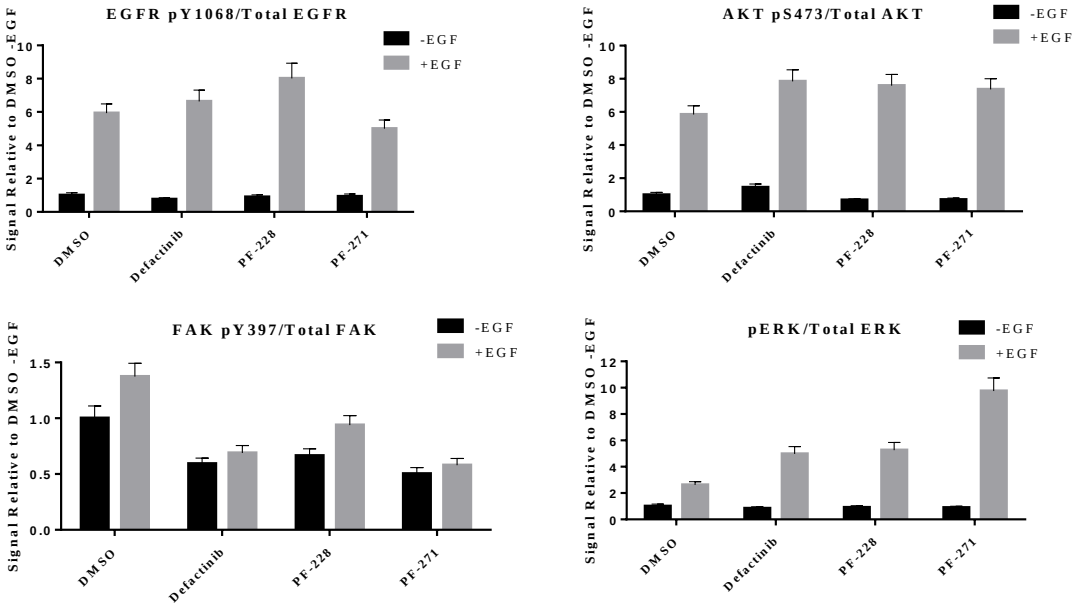

B A549 Quantification

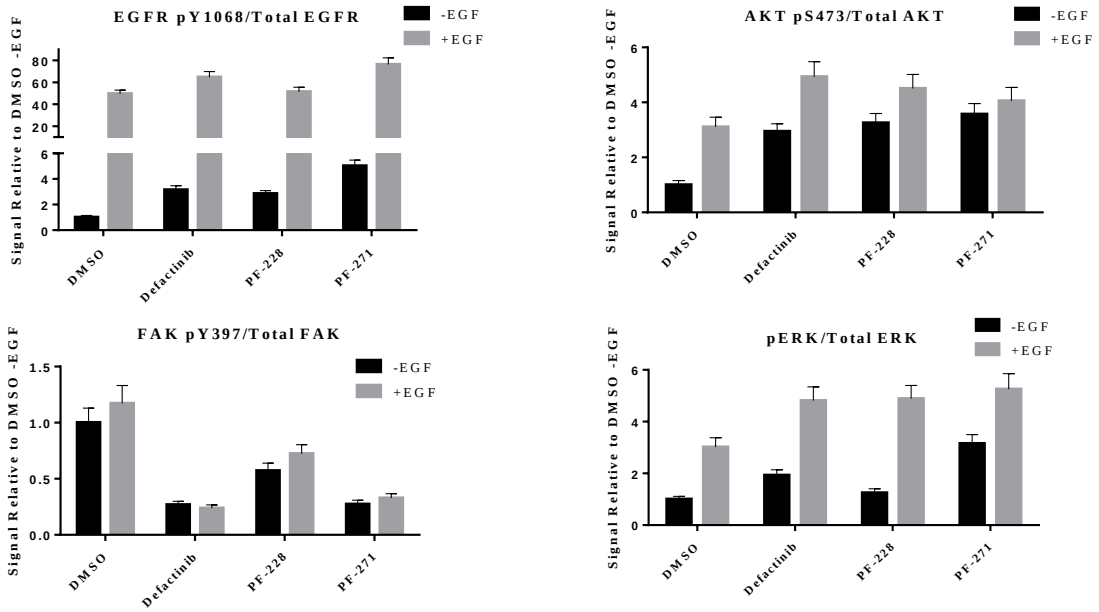

Fig. S2. Quantification of H292 and A549 immunoblot experiments from Fig. 1. Densitometry analysis from experiments in EGFR-positive **(A)** H292 and **(B)** A549 lung cancer cells relative to DMSO –EGF control. Results shown are averaged results from three independent experiments, with error bars represented as standard deviations. Two-way ANOVA statistical analysis is shown in Supplemental File 2.

Fig. # S3:

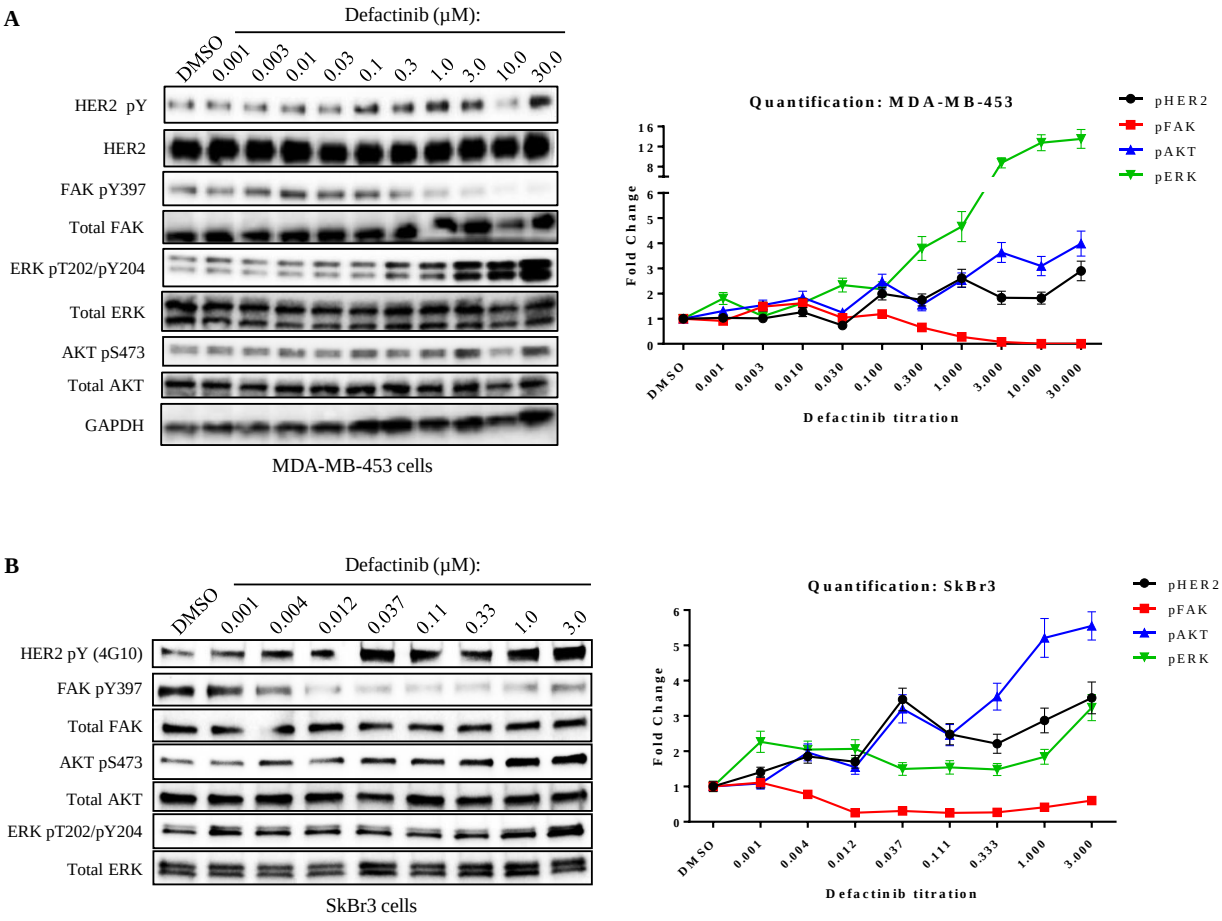

Fig. S3. **Defactinib-induced rapid compensatory RTK reprogramming in HER2-positive cells is dose-dependent and correlates with loss of FAK phosphorylation. (A)** MDA-MB-453 and **(B)** SkBr3 HER2^{+} breast cancer cells were treated with indicated concentration of defactinib for 1 hour. Images shown are representative of three independent experiments. Densitometry analysis is shown on the right panel. Note, as FAK pY397 levels start to decrease, compensatory increases in pHER2, pERK, and pAKT are detected. Additionally, in SkBr3 cells, FAK pY397 levels start to increase at higher doses of defactinib and higher levels of pHER2.

Fig. # S4:

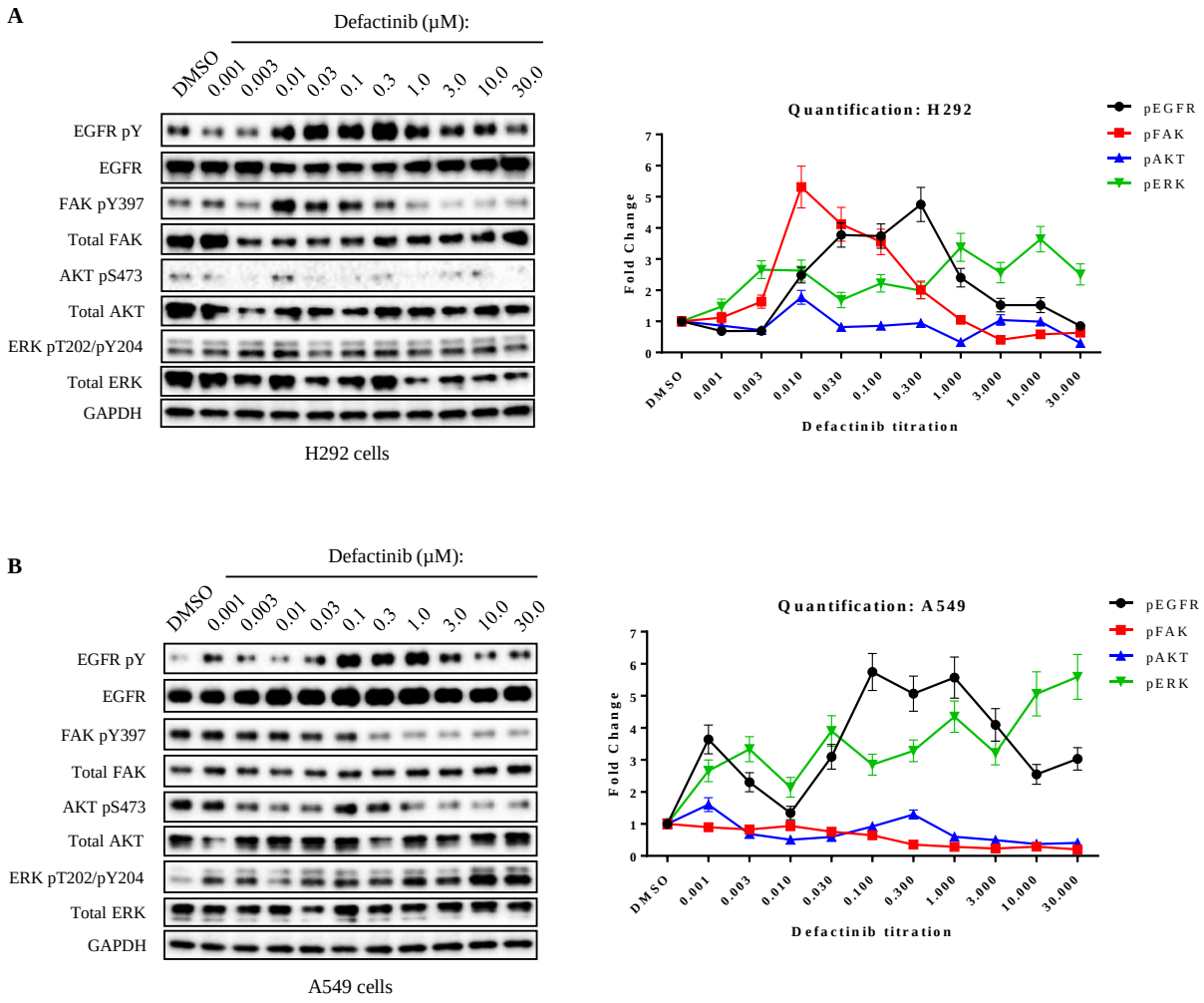

Fig. S4. **Defactinib-induced rapid compensatory RTK reprogramming in EGFR-positive cells occurs at low doses. (A)** H292 and **(B)** A549 EGFR^{+} breast cancer cells were treated with indicated concentration of defactinib for 1 hour. Images shown are representative of three jindependent experiments. Densitometry analysis is shown on the right panel. Note, even at low doses (< 1 μM) of defactinib, compensatory increases in pEGFR are observed. Intriguingly, 0.01-0.3 μM defactinib treatment causes hyperphosphorylation of FAK at Y397 in H292 cells.

Fig. # S5:

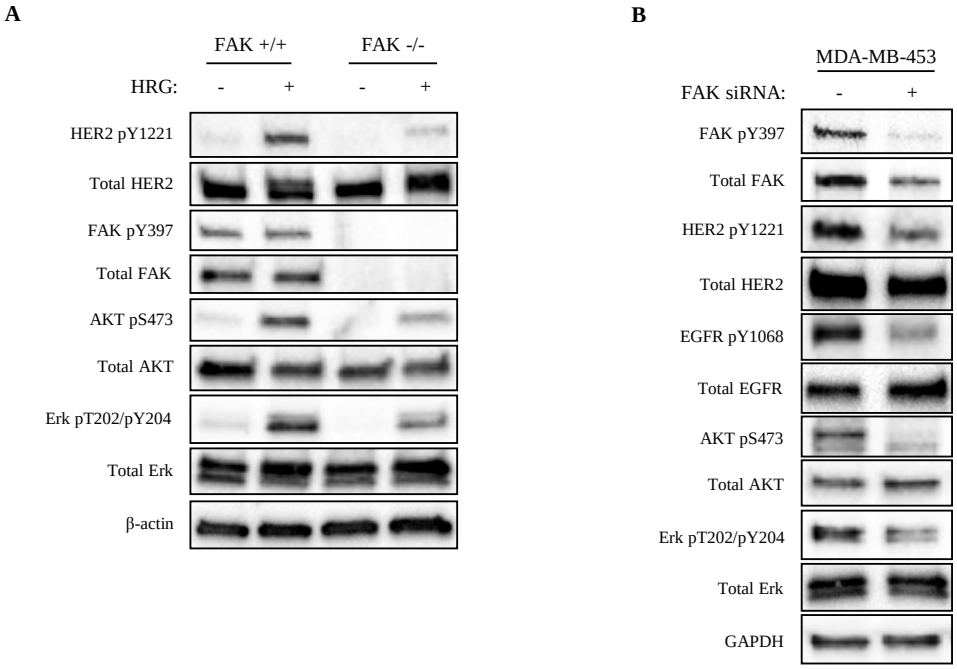

Fig. S5. Total FAK levels regulate downstream activation of AKT/ERK pathways in HER2 positive cells. (A) Immunoblot using HER2/HER3-positive FAK -/- and FAK +/+ MEFs. Cells were serum-starved overnight followed by HRG stimulation for 30 min. Note: FAK-depleted MEFs showed a reduced capacity to activate HER2, AKT, and ERK after HRG stimulation. **(B)** Immunoblot using HER2-positive MDA-MB-453 breast cancer cells and FAK-specific siRNA. Cells were transfected with siRNA for 24 hours and subsequently lysed for immunoblot analysis. Note: FAK siRNA transfected cells showed lower levels of HER2, EGFR, AKT, and ERK phosphorylation. Images shown are representative of three independent experiments.

Fig. # S6:

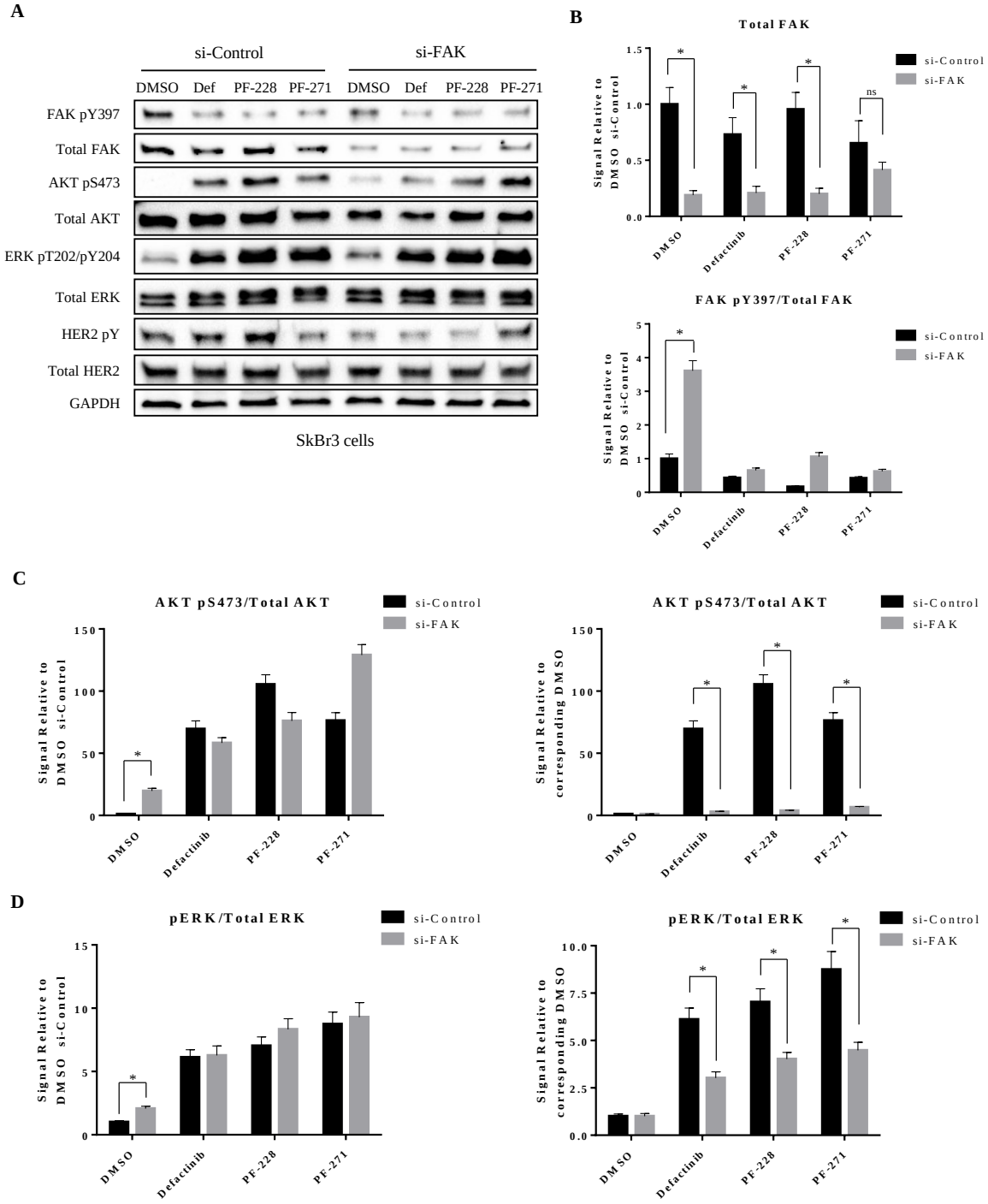
A
si-Control
si-FAK
DMSO
Def
PF-228
PF-271
DMSO
Def
PF-228
PF-271
FAK pY397
Total FAK
AKT pS473
Total AKT
ERK pT202/pY204
Total ERK
HER2 pY
Total HER2
GAPDH
SkBr3 cells
B
Total FAK
Signal Relative to DMSO si-Control
si-Control
si-FAK
*
*
*
ns
DMSO
Defactinib
PF-228
PF-271
FAK pY397/Total FAK
Signal Relative to DMSO si-Control
si-Control
si-FAK
*
DMSO
Defactinib
PF-228
PF-271
C
AKT pS473/Total AKT
Signal Relative to DMSO si-Control
si-Control
si-FAK
*
DMSO
Defactinib
PF-228
PF-271
AKT pS473/Total AKT
Signal Relative to corresponding DMSO
si-Control
si-FAK
*
*
*
DMSO
Defactinib
PF-228
PF-271
D
pERK/Total ERK
Signal Relative to DMSO si-Control
si-Control
si-FAK
*
DMSO
Defactinib
PF-228
PF-271
pERK/Total ERK
Signal Relative to corresponding DMSO
si-Control
si-FAK
*
*
*
DMSO
Defactinib
PF-228
PF-271

Fig. S6. FAK knockdown by siRNA in SkBr3 cells reduces FAK kinase inhibitor-induced RTK reprogramming. (A) Immunoblots showing effect of FAK knockdown on FAK kinase inhibitor-induced RTK reprogramming. Serum-starved SkBr3 cells were transfected with si-Control or si-FAK sequence and subsequently treated with 10μM FAK-kinase inhibitor (defactinib, PF-228, PF-271) for 1 hour. Results are representative of three independent experiments. **(B)** Densitometry analysis of total FAK and FAK pY397 levels. Upper panel: a statistical significant decrease in total FAK levels was detected in DMSO, defactinib, and PF-228 treatment groups. Lower panel: FAK pY397/total FAK ratio levels. Note: FAK siRNA increased FAK pY397/total FAK levels, indicated a compensatory feedback to maintain pY397 levels. **(C)** Densitometry analysis of AKT pS473/total AKT levels. Upper panel: AKT pS473/total AKT relative to DMSO si-Control. Note: FAK siRNA alone induces compensatory increases in pAKT. Lower panel: AKT pS473/total AKT relative to corresponding DMSO control. Note: FAK siRNA reduces FAK kinase inhibitor-induced activation of AKT. **(D)** Densitometry analysis of ERK pT202-pY204/total ERK levels. Upper panel: pERK/total ERK relative to DMSO si-Control. Note: FAK siRNA alone induces compensatory increases in pERK. Lower panel: pERK/total ERK relative to corresponding DMSO control. Note: FAK siRNA reduces FAK kinase inhibitor-induced activation of ERK. Two-way ANOVA statistical analysis was performed for all densitometry measurements. Asterisks represent multiple comparison corrected p-values < 0.05.

Fig. # S7:

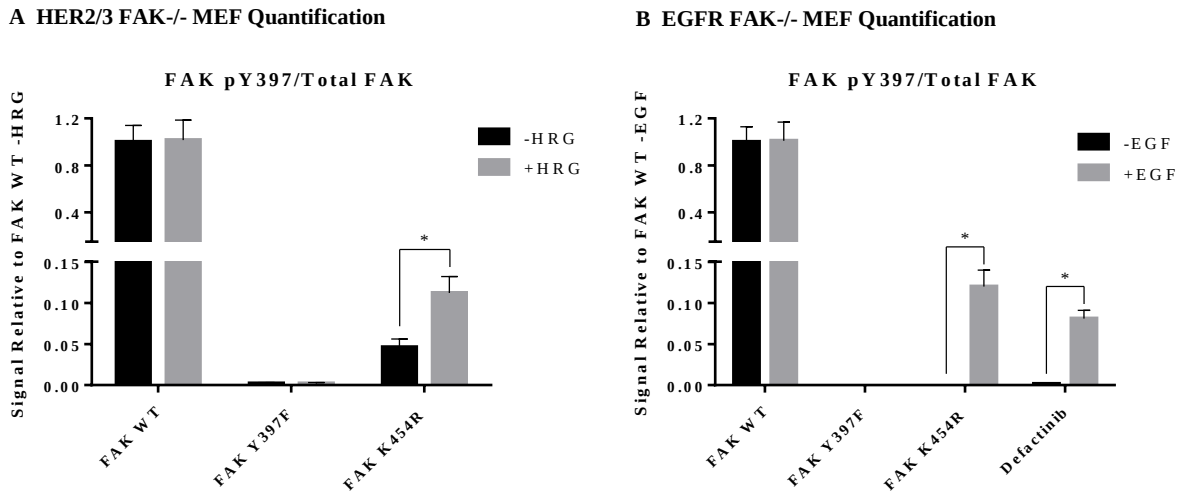

Fig. S7. Quantification of immunoblot experiments from Fig. 2. FAK pY397/total FAK densitometry analysis from experiments in **(A)** HER2/HER3-positive FAK -/- MEFs and **(B)** EGFR-positive FAK-/- MEFs relative to FAK WT –HRG/EGF control. Note: GF stimulation partially reactivates either kinase-dead (K454R) or defactinib-inhibited FAK. Results shown are averaged results from three independent experiments, with error bars represented as standard deviations. Student T-test statistical analysis was performed to identify differences between -GF/+GF groups. Asterisks represent p-values < 0.05.

Fig. # S8:

Fig. S8. **Src is not required for FAK transphosphorylation downstream of HER2**. **(A)** Immunoblot showing the absence of SRC from SRC/YES/FYN-null (SYF-) cells compared to SRC expressing 293T cells. **(B)** Phosphorylation of FAK at Y397 in SYF- & SYF- stably expressing HER2/HER3 following Heregulin-β1 (HRG) stimulation (30 min) in the presence of defactinib (1h).

Fig. #S9:

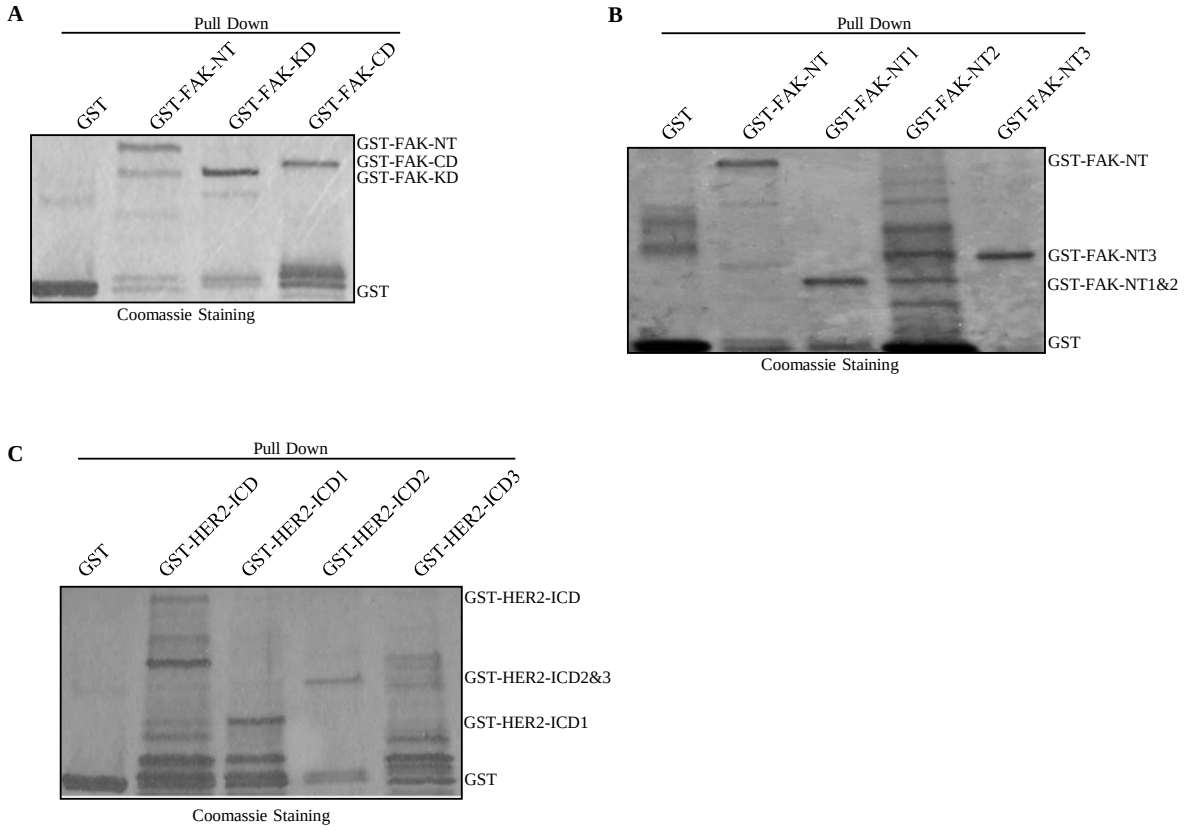

Fig. S9. **Coomassie-staining confirmation of protein loading in GST pull-down assays. (A)** Loading of GST, GST-FAK-NT, GST-FAK-KD, and GST-FAK-CD proteins utilized in Fig. 3A. **(B)** Loading of GST, GST-FAK-NT, GST-FAK-NT1, GST-FAK-NT2, and GST-FAK-NT3 proteins utilized in Fig. 3B. **(C)** Loading of GST, GST-HER2-ICD, GST-HER2-ICD1, GST-HER2-ICD2, and GST-HER2-ICD3 utilized in Fig. 3B.

Fig. #S10:

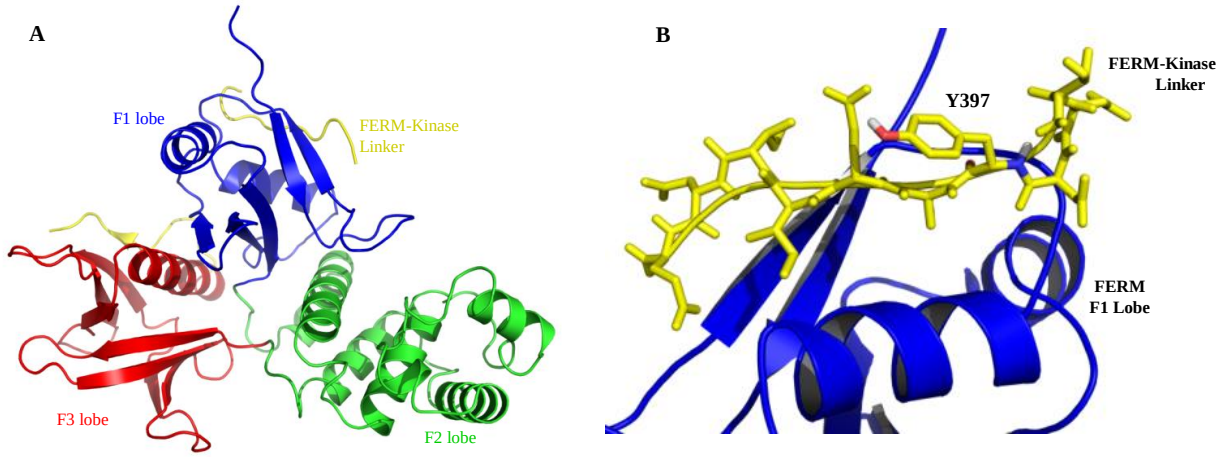

Fig. S10. **X-ray crystal structure of the FAK FERM domain and proximity of the Y397 linker region (AA 394-403) to the FERM F1 lobe. (A)** Crystal structure of the FAK FERM domain (PDB 2AL6). The F1 lobe (blue), F2 lobe (green), F3 lobe (red), and FERM-kinase linker (yellow) of the FAK FERM domain are depicted. **(B)** Proximity of Y397, part of the FERM-kinase linker region (yellow), to the FAK FERM F1 lobe (blue). Note, Y397 is within a 10-residue linear sequence (AA 394-403) that binds back onto the FAK FERM F1 lobe.

Fig. #S11:

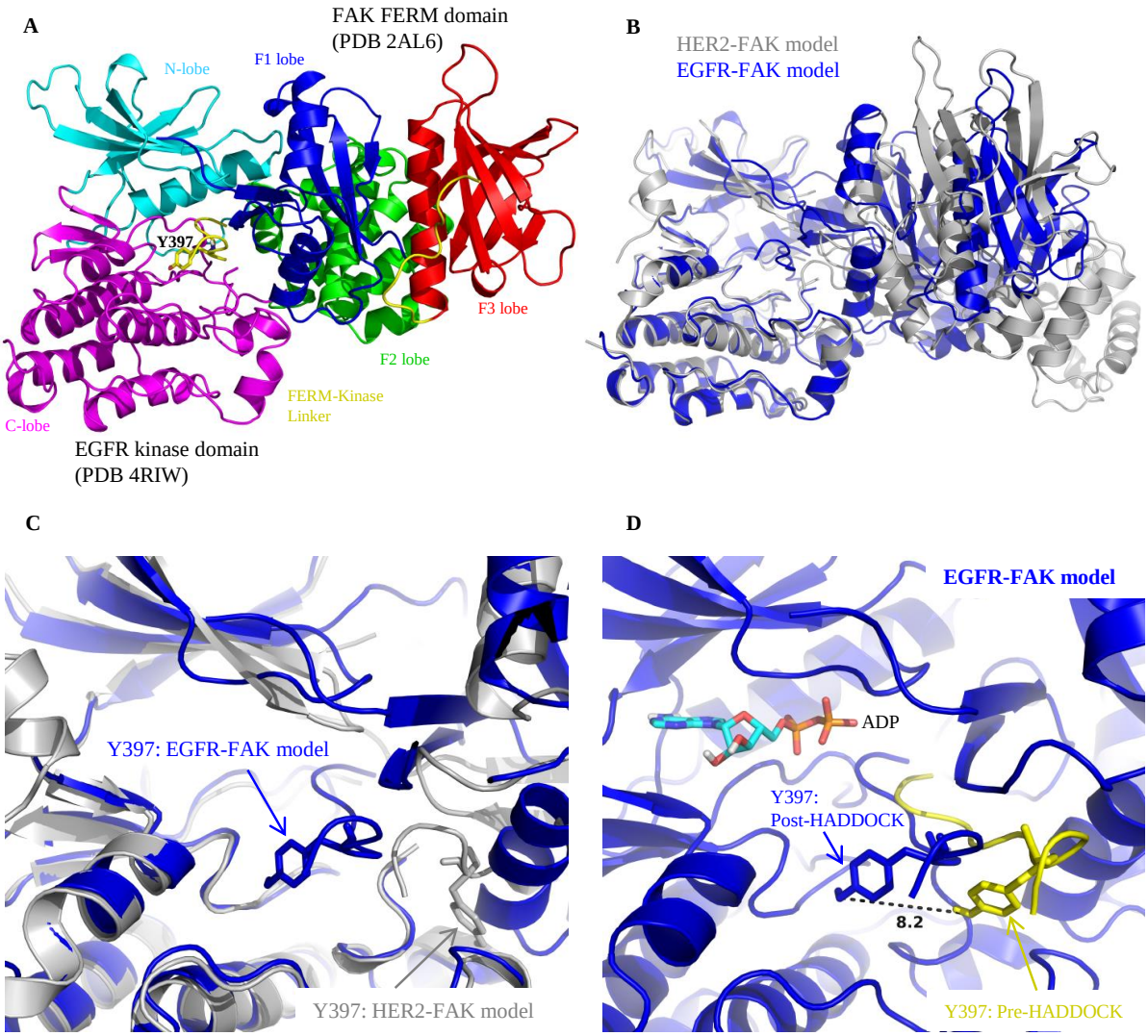

Fig. S11. EGFR-FAK HADDOCK docking studies. (A) Structural model of the EGFR-FAK interaction as determined by HADDOCK docking studies. The N-lobe (cyan) and C-lobe (magenta) of the EGFR kinase domain (PDB 4RIW) as well as the F1 lobe (blue), F2 lobe (green), F3 lobe (red), and FERM-kinase linker (yellow) of the FAK FERM domain (PDB 2AL6) are depicted. The model shown represents the top-ranked cluster in HADDOCK. **(B)** Structural alignment of the top HER2-FAK (gray) and EGFR-FAK (blue) HADDOCK models using PyMOL. Alignment indicates similarities between models, however non-identical binding

positions of the FERM domain. **(C)** Similarities in FAK Y397 location between HER2-FAK (gray) and EGFR-FAK (blue) models. Note, both models predict Y397 binding to kinase substrate-binding regions and direct phosphorylation. **(D)** Dynamic nature of the FAK Y397 linker region and flexibility within the EGFR kinase domain pocket upon EGFR-FAK binding. Structural alignment was performed with the FAK FERM pre-HADDOCK docking structure (yellow) and compared to the post-HADDOCK induced-fit structure (blue). A significant shift in Y397 location (8.2Å) was observed towards bound ADP in the ATP-binding pocket, supporting dynamic character of Y397 region upon EGFR-FAK binding in order to undergo phosphorylation.

Fig. #S12:

A

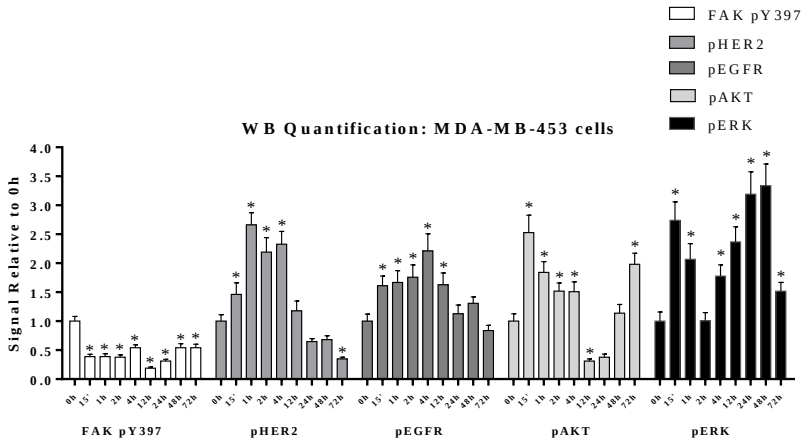
FAK pY397
pHER2
pEGFR
pAKT
pERK
WB Quantification: MDA-MB-453 cells
Signal Relative to 0h
FAK pY397
pHER2
pEGFR
pAKT
pERK

B

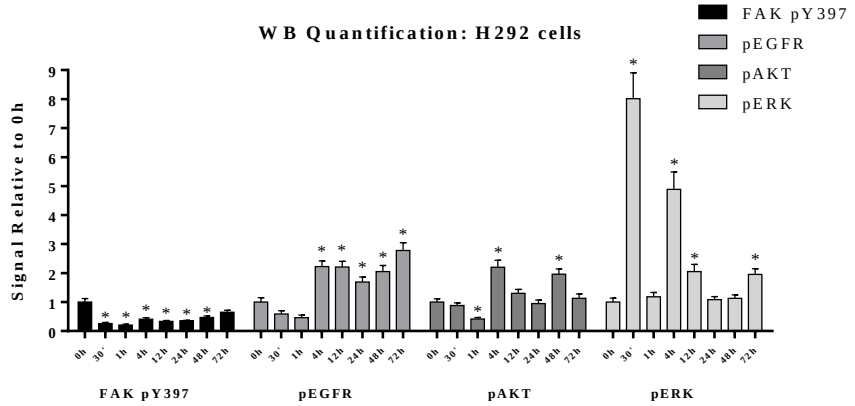
FAK pY397
pEGFR
pAKT
pERK
WB Quantification: H292 cells
Signal Relative to 0h
FAK pY397
pEGFR
pAKT
pERK

C

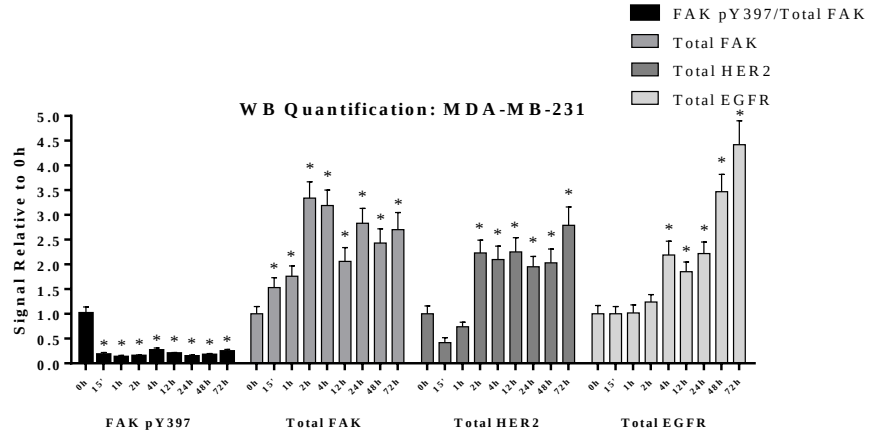
FAK pY397/Total FAK
Total FAK
Total HER2
Total EGFR
WB Quantification: MDA-MB-231
Signal Relative to 0h
FAK pY397
Total FAK
Total HER2
Total EGFR

Fig. S12. Quantification of immunoblot experiments from Fig. 5. FAK pY397, pEGFR, pHER2, pAKT, pERK, total FAK, total EGFR, and total HER2 densitometry analysis from Fig. 5 experiments in **(A)** MDA-MB-453, **(B)** H292, and **(C)** MDA-MB-231 cells. Results shown are averaged results from three independent experiments, with error bars represented as standard deviations. Two-way ANOVA statistical analysis was performed to identify differences between 0h and all other timepoints. Asterisks represent multiple comparison corrected p-values < 0.05.

Fig. #S13:

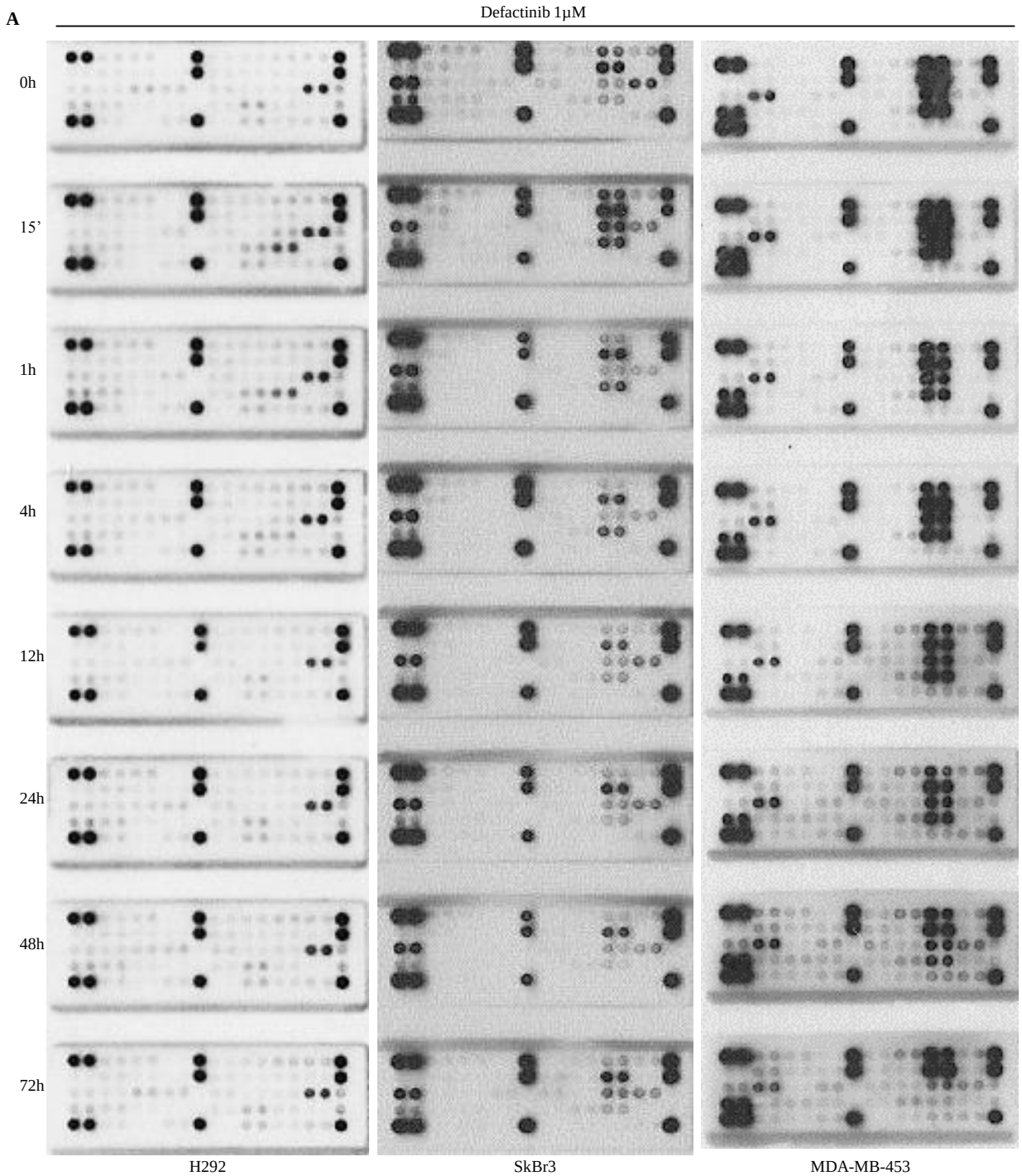
A
Defactinib 1µM
0h
15'
1h
4h
12h
24h
48h
72h
H292
SkBr3
MDA-MB-453

Fig. S13. RTK arrays of RTK^{High} cell lines treated with defactinib. Results from RTK arrays in **(A)** H292 (EGFR^{+}), SkBr3 (HER2^{+}), and MDA-MB-453 (HER2^{+}) cancer cell lines. Cells were treated with defactinib for the indicated timepoints and analyzed as described in the Materials and Methods. Note, images represent 20 sec of exposure time. ERK is activated after 15 min of defactinib treatment in all three cell lines and S6 ribosomal protein is activated after 15min in H292 and SkBr3 cells.

Fig. #S14:

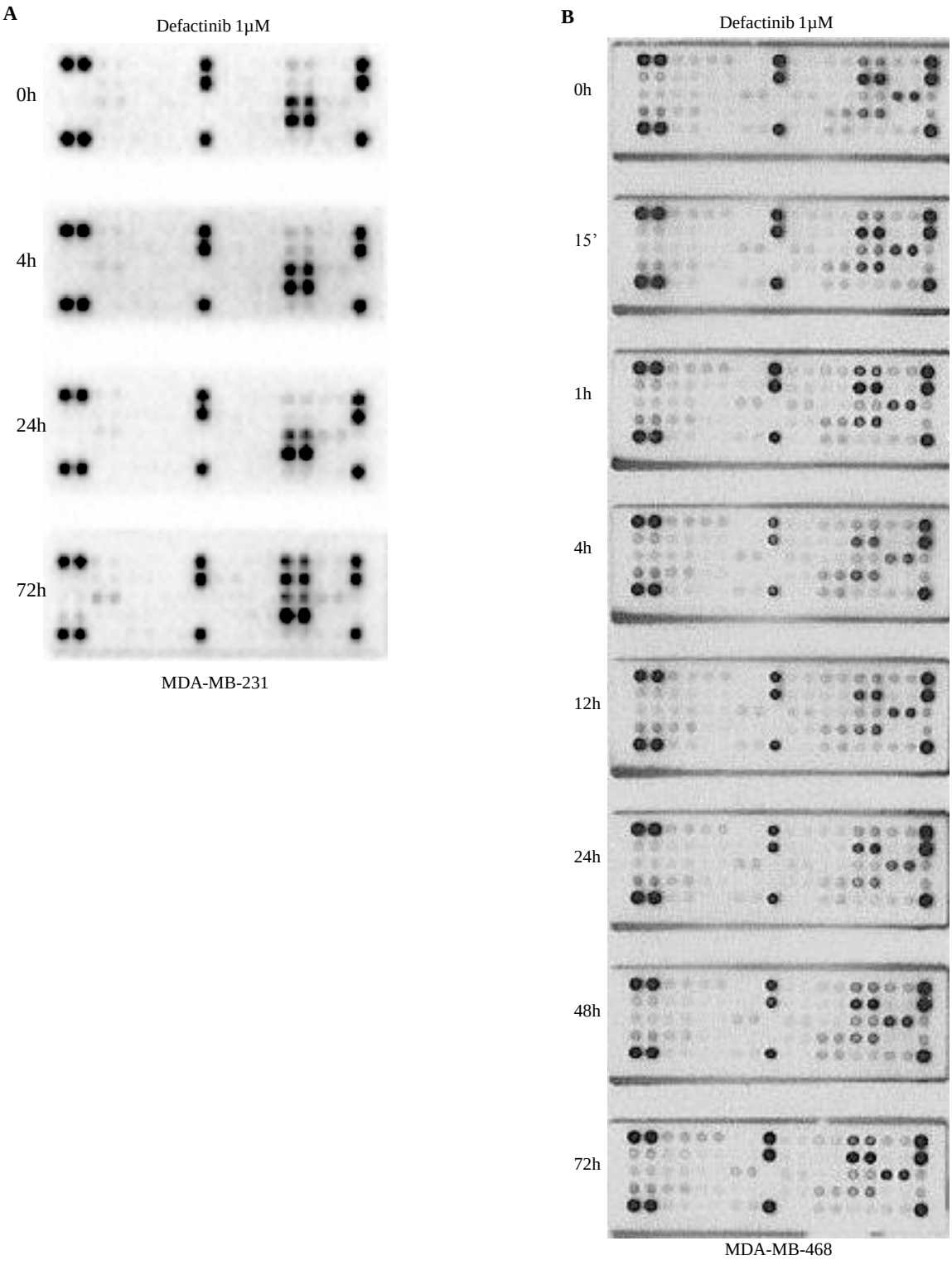
A
Defactinib 1µM
0h
4h
24h
72h
MDA-MB-231
B
Defactinib 1µM
0h
15’
1h
4h
12h
24h
48h
72h
MDA-MB-468

Fig. S14. RTK arrays of RTK^{Low} cell lines treated with defactinib. Results from RTK arrays in **(A)** MDA-MB-231 cells and **(B)** MDA-MB-468 cells. Cells were treated with defactinib for the indicated timepoints and analyzed as described in the Materials and Methods. Note, images represent 20 sec of exposure time.

Fig. #S15:

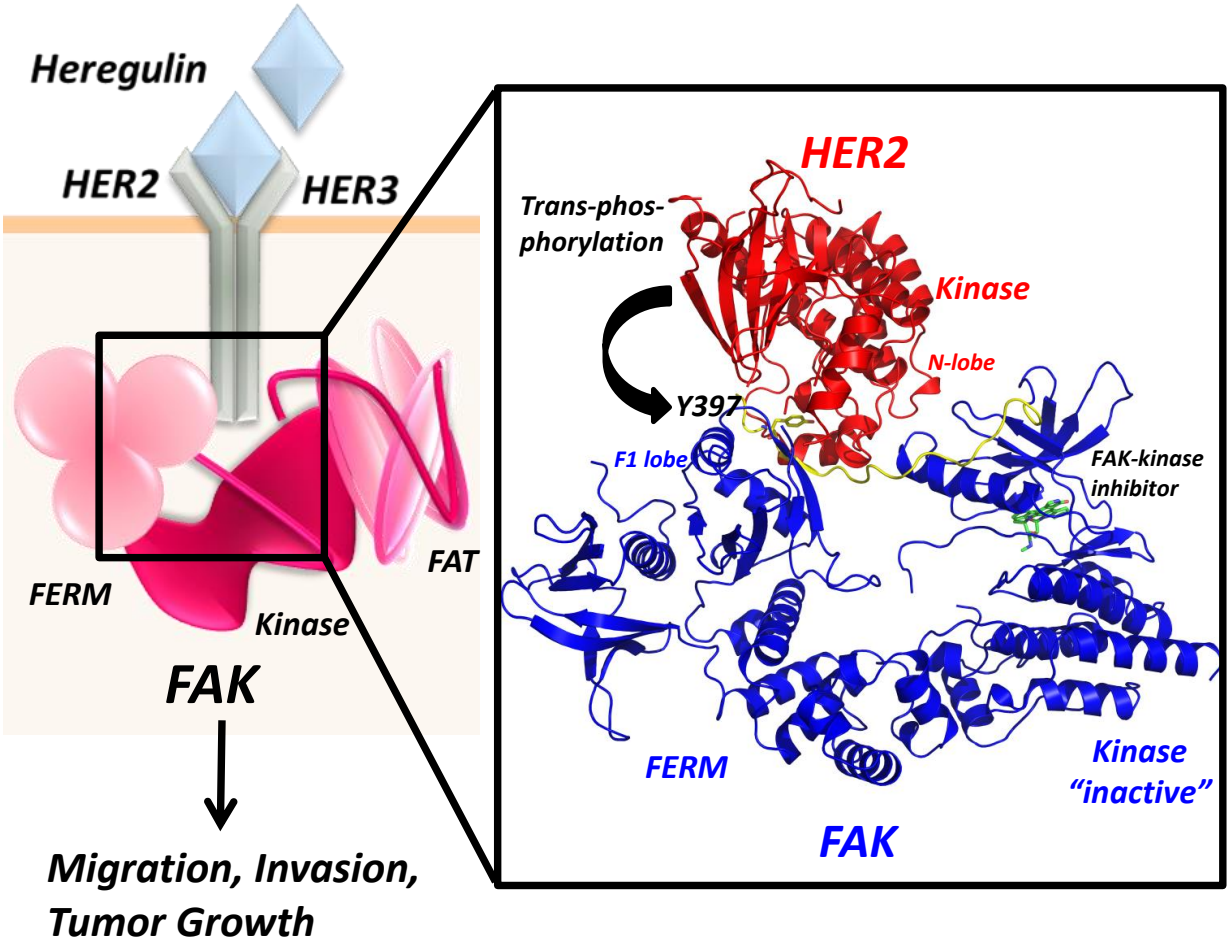

Fig. S15. Overview of the FAK-kinase inhibitor drug resistance pathway through transphosphorylation of Y397 by HER2. The diagram on the left describes the FAK reactivation pathway by HER2 and other RTKs. Upon FAK-kinase inhibition, HER2 is upregulated (by both phosphorylation and expression) to maintain FAK phosphorylation and therefore FAK-dependent tumorigenic functions (migration, invasion, and tumor growth). The HADDOCK structural model on the right (adapted from PDB 2J0J) describes the structural significance of HER2-FAK interaction in drug resistance to FAK-kinase inhibitors. Inhibition of FAK catalytic activity (kinase inhibitor-green) promotes the auto-inhibitory conformation of

FAK, where Y397 is bound to the F1 lobe of the FERM domain. As a compensatory mechanism, HER2 binds to the F1 lobe and re-phosphorylates FAK Y397 through direct transphosphorylation in order to reactivate FAK downstream pathways. Direct Y397 inhibitors which disrupt both auto- and trans-phosphorylation pathways may evade RTK-dependent drug resistance and increase the therapeutic potential of FAK inhibitors.